

****FULL TITLE****
*ASP Conference Series, Vol. **VOLUME**, **YEAR OF PUBLICATION***
****NAMES OF EDITORS****

Spitzer Massive Lensing Cluster Survey

E. Egami¹, G. H. Rieke¹, J. R. Rigby¹, C. Papovich¹, J.-P. Kneib²,
 G. P. Smith³, E. Le Floch¹, K. A. Misselt¹, P. G. Pérez-González¹,
 J.-S. Huang⁴, H. Dole⁵, & D. T. Frayer⁶

(1) *Univ. of Arizona*, (2) *Laboratoire d'Astrophysique de Marseille*, (3)
Caltech, (4) *CfA*, (5) *Institut d'Astrophysique Spatiale*, (6) *SSC*

Abstract. We are currently undertaking a *Spitzer* GTO program to image ~ 30 massive lensing clusters at moderate redshift with both IRAC and MIPS. By taking advantage of the gravitational lensing power of these clusters, we will study the population of faint galaxies that are below the nominal *Spitzer* detection limits. Here, we present a few examples of our science programs.

1. Introduction

The gravitational lensing power of massive galaxy clusters can be exploited to improve the nominal *Spitzer* detection limits. Clusters at $z = 0.2 - 0.4$ typically magnify a background sky area of ~ 1 arcmin² with a magnification factor of $\gtrsim 5$ and often up to 20–30, which directly translates into a gain in the signal-to-noise ratio. Furthermore, if the sensitivity is limited by source confusion, gravitational lensing offers a further benefit of reducing the confusion noise by spreading out the background galaxies. For these reasons, *Spitzer* imaging of massive cluster fields could potentially achieve a depth that is not attainable even in the GOODS fields. In the past, the effectiveness of such a strategy was anticipated for submillimeter observations (Blain 1997), and was successfully demonstrated by a series of SCUBA cluster observations (e.g., Smail et al. 2002).

Motivated by this potential and the success of the submillimeter cluster surveys, we are currently undertaking a *Spitzer* GTO program to image ~ 30 massive clusters with both IRAC and MIPS. The main target selection criteria are the following: (1) X-ray luminous, i.e., massive ($L_X > 7 \times 10^{44}$ erg/s); (2) moderate redshift ($z \sim 0.15 - 0.5$); (3) low IR background ($N_H < 3.5 \times 10^{22}$ cm⁻²); and (4) abundance of ancillary data (e.g., *HST* images, which are necessary to construct accurate cluster mass models). All the clusters will be imaged in the four IRAC bands and in the MIPS 24 μ m band; MIPS 70 and 160 μ m observations will be carried out for ~ 10 clusters.

Such a rich data set provides opportunities for many exciting scientific projects. Here, we will present a few examples, concentrating on the lensed sources. In a parallel effort, cluster galaxy evolution is also being studied in combination with a sample of local and high-redshift ($z \sim 1$) clusters.

2. 24 μ m Sources in the Cluster Cores

Lensing clusters are especially useful for deep imaging at 24 μ m because the cluster cores, where the lensing magnification is strongest, are dominated by

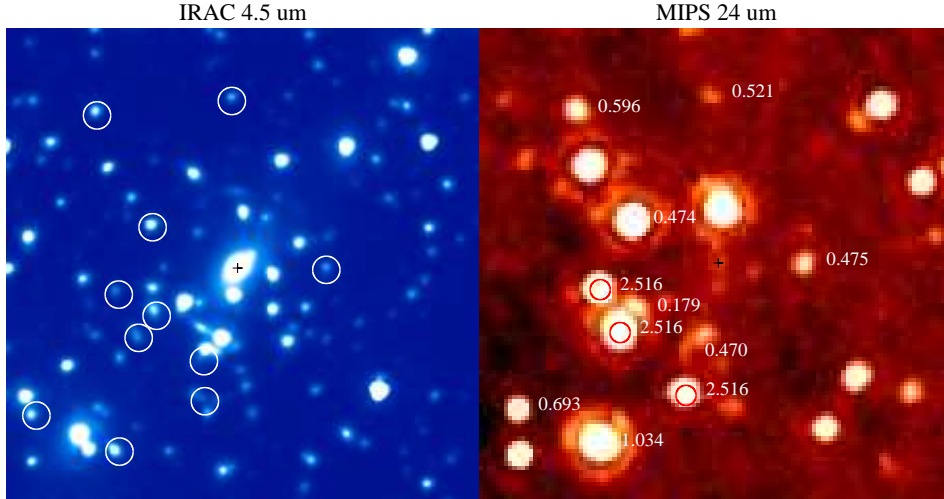


Figure 1. Spitzer images of Abell 2218: Left – IRAC 4.5 μm image. Galaxies with spectroscopic redshifts (Ebbels et al. 1998) are marked with circles; Right – MIPS 24 μm image. The spectroscopic redshifts are listed. The triply lensed images of the $z \sim 2.5$ submillimeter galaxy (Kneib et al. 2004a) are marked with circles. In both images, the position of the cD galaxy is marked with a cross.

early-type galaxies, which are faint at 24 μm . As shown in Figure 1, the majority of the 24 μm sources seen in the cluster core are background lensed sources.

Scientifically, the driver here is to study the population of faint 24 μm galaxies which are below the detection limit of field deep surveys. Most recently, the evolution of 24 μm -selected galaxies have been investigated up to $z = 1$ (Le Floc’h et al. 2005) and to $z = 2.5$ (Pérez-González et al. 2005) based on the Spitzer GTO deep survey data of CDF-S and HDF-N using both spectroscopic and photometric redshifts. However, these 24 μm data are not quite deep enough to constrain the shape of the luminosity function below L^* at $z \gtrsim 1$. Furthermore, many of the high-redshift 24 μm galaxies are too faint to detect at 70 and 160 μm , making it impossible to determine their total IR luminosities directly. This cluster program should help address these problems by detecting fainter 24 μm sources and by increasing 70/160 μm detections.

Figure 1 also shows the detection of the triply lensed $z \sim 2.5$ submm galaxy discovered by Kneib et al. (2004a). The three lensed images are faint in the optical, but they are clearly detected in all four IRAC bands and are fairly bright at 24 μm (though still below 1 mJy). Curiously, the spectral energy distribution (SED) measured by IRAC is different from what we saw with the submillimeter/radio sources in the Lockman Hole (Egami et al. 2004). Considering that this source has a high magnification (a total of $\times 45$ with all three images) and that each image further breaks up into substructures with different colors, the IRAC SED might be distorted by differential magnification.

Although most cD galaxies are faint at 24 μm as is the case with Abell 2218, a few cD galaxies in the so-called cooling flow clusters show 24 μm luminosities one to two orders of magnitude larger than those of average cD galaxies. This indicates that these cD galaxies harbor a luminosity source which is blocked from our view at shorter wavelengths.

3. Properties of Stellar Populations at $z = 4 - 5$ and Beyond

The Balmer/4000Å breaks get redshifted into the K band at $z \sim 4$. Therefore, to determine the properties of the underlying stellar population for galaxies at $z \gtrsim 4$ (e.g., age, mass), it is essential to measure fluxes redward of the K -band. Presently, IRAC is the only instrument that is sensitive enough to provide such information.

Figure 2 shows the IRAC 3.6 μm detections of three galaxies with spectroscopic redshifts of 4.5 – 5. The magnification factors estimated for these galaxies range from 7 to 10, suggesting that these galaxies would not have been detected without the cluster lensing.

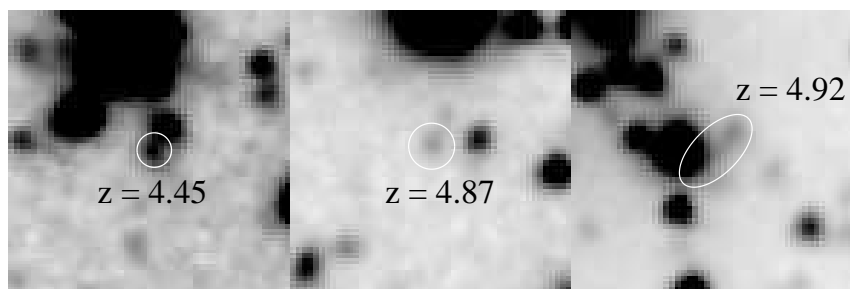


Figure 2. IRAC 3.6 μm images of three galaxies at $4 < z < 5$: Left – $z = 4.45$ galaxy in Abell 2219; Middle – $z = 4.87$ galaxy in Abell 1689; Right – $z = 4.92$ galaxy in MS1358. The first two redshifts are from Frye, Broadhurst, & Benítez (2002) while the third one is from Franx et al. (1999).

The remarkable potential of *Spitzer* to probe even higher redshift was demonstrated dramatically by the IRAC detection of a gravitationally lensed $z \sim 7$ galaxy at 3.6 and 4.5 μm (Egami et al. 2005). This galaxy was first discovered by Kneib et al. (2004b), and is located in the cluster Abell 2218 (Figure 1). Figure 3 shows the *HST*/NICMOS and *Spitzer*/IRAC images of the lensed pair. It

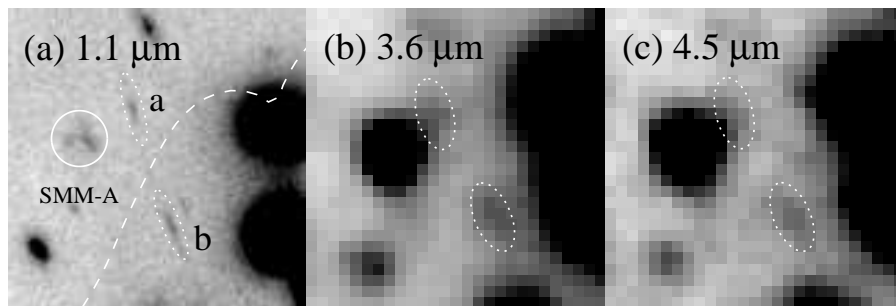


Figure 3. *HST*/NICMOS and *Spitzer*/IRAC images of the $z \sim 7$ lensed pair: (a) NICMOS 1.1 μm image. Components *a* and *b* as well as the $z \sim 2.5$ submillimeter source SMM-A (the northernmost of the three lensed images in Figure 1) are marked. The dashed line indicates the $z \geq 6.5$ critical lines; (b) IRAC 3.6 μm image; (c) IRAC 4.5 μm image.

is located symmetrically with respect to the critical lines for background sources at $z \geq 6.5$, suggesting that the redshift must be at least this high.

Figure 4 compares the SED of component *b* with a range of models. Although the redshift has not been confirmed spectroscopically, photometric redshifts derived from Figure 4 range from 6.6 to 6.8, consistent with the lower limit set by the lens model. The figure clearly illustrates the power of IRAC to measure the flux longward of the Balmer break for such a high-redshift galaxy. For this galaxy, we concluded that its underlying stellar population is in the post-starburst stage with an age of at least ~ 50 Myr (and quite possibly a few hundred Myr), suggesting that a mature system is already in place at this early era. The stellar mass is $\sim 10^9 M_{\odot}$, an order of magnitude smaller than typical Lyman break galaxies at $z = 3 - 4$.

Considering that this galaxy appears to be in the poststarburst stage, its predecessor is likely to be more luminous at higher redshift, mitigating perhaps the effect of the increased luminosity distance. This presents a further exciting possibility that we may be yet to witness even higher redshift galaxies with *Spitzer*.

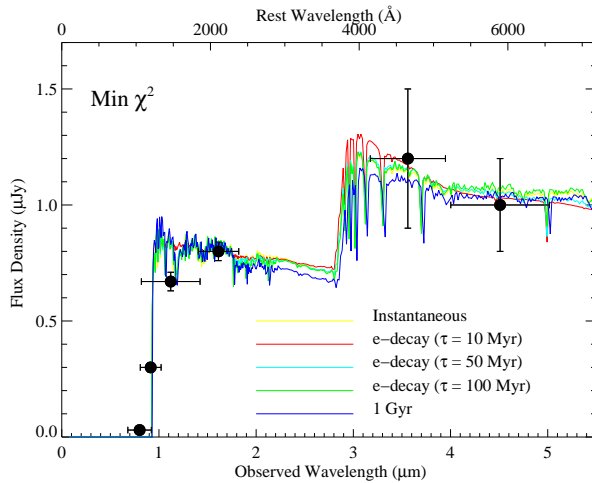


Figure 4. SED model fits to the observed SED of the $z \sim 7$ galaxy (component *b*). The best (i.e., minimum χ^2) model for each star formation history is plotted. The rest-frame wavelength at $z = 6.65$ is also shown. The measured flux at $1.1 \mu\text{m}$ is expected to be significantly lower than the true continuum level because the F110W filter passband extends below 1216 \AA in the restframe. The intrinsic flux densities (i.e., without the magnification) is estimated to be 25 times lower.

References

- Blain, A. W. 1997, MNRAS, 290, 553
 Ebbels, T., Richard, R. S., Kneib, J.-P., Le Borgne, J.F., Pelló, R., Smail, I., & Sanahuja, B. 1998, MNRAS, 295, 75
 Egami, E., et al. 2004, ApJS, 154, 130
 Egami, E., et al. 2005, ApJ, 618, L5
 Franx, M., Illingworth, G.D., Kelson, D.D., van Dokkum, P.G., & Tran, K.-V. 1997, ApJ, 486, L75
 Frye, B., Broadhurst, T., & Benítez, N. 2002, ApJ, 568, 558
 Kneib, J.-P., van der Werf, P. P., Knudsen, K. K., Smail, I., Blain, A., Frayer, D., Barnard, V., & Ivison, R. 2004a, MNRAS, 349, 1211
 Kneib, J.-P., Ellis, R. S., Santos, M. R., & Richard, J. 2004b, ApJ, 607, 697
 Le Floc'h, E., et al. 2005, this volume
 Pérez-González, P. G., et al. 2005, this volume
 Smail, I., Ivison, R. J., Blain, A. W., & Kneib, J.-P. 2002, MNRAS, 331, 495